E-textile based Wavy Surface WPT Flexible Antenna with Frequency Self-reconfiguration Function for Battery-less Sensor Platform

Jinhyoung Kim, Cheolung Cha, Kwonhong Lee, Jungsuek Oh, *Senior Member, IEEE,* Yongtaek Hong

***Abstract*—This paper is a study on the center frequency reconfiguration of a flexible antenna. In the case of a flexible antenna, the center frequency shifts due to parasitic components generated when the antenna is bent. In previous studies, research has been conducted to reconfigurate the center frequency through a reconfiguration circuit. When using a reconfiguration circuit, it is difficult to flexibly configure all systems due to increased complexity. Therefore, in this paper, we propose a flexible antenna that does not change the center frequency even when the antenna is bent through a wavy surface structure without the aid of a frequency reconfiguration circuit. By studying the parasitic component that occurs when the antenna is bent, the cause of the change in the center frequency is identified and a structure to solve it is proposed. In order to calculate the parasitic component, an approximate model divided by the vertical component of the bending surface of the flexible antenna was used. In this paper, a gating air-gap structure was proposed to realize a wavy surface, and through this, the antenna gain was increased by 1.47 dBi. In addition, through the wavy surface structure using E-textile, it was possible to reduce the frequency shift by about 86% (70 MHz to 10 MHz) and improve the gain reduction by about 86% (4.4 dBi to 0.63 dBi). This allows the frequency to be reconfigured in real time without additional circuitry.**

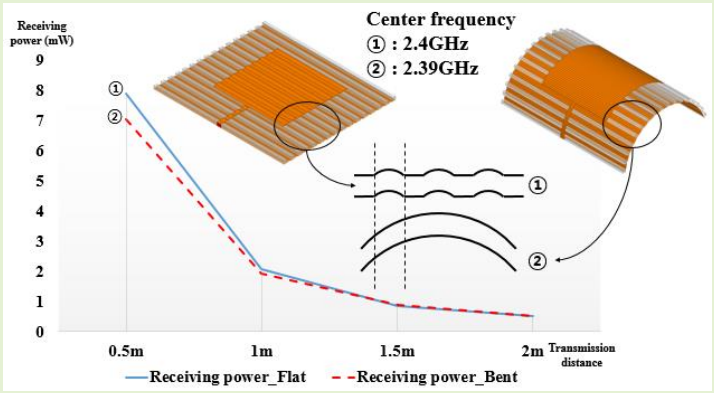

***Index Terms*— Flexible antenna, frequency self-reconfiguration, wavy surface antenna, gridded substrate, wireless power transfer, battery-less sensor platform, strain sensor.**

I. Introduction

WERABLE devices are growing more and more over time. According to Cisco, the number of wearable devices is estimated to exceed 1.1 billion by 2022 [1]. Wearable devices are electronic devices that are worn on a part or all of the body to measure bio-factors such as body temperature and blood pressure as well as the wearer's posture and movement. Therefore, it is not limited to wrist watches and fitness bands, but is used in various medical applications [2], [3]. Such wearable devices are composed of sensors, communication devices, antennas, and batteries. In particular, an antenna is essential to transfer the acquired information to an external device. The wearable antenna is manufactured using flexible materials such as polydimethylsiloxane (PDMS) [4] and conductive cloth [5], [6] to reduce the sense of rejection with the human body.

When designing a flexible antenna for wearables, various points such as flexibility, strength, and interference with the human body [7] are considered, but inevitably, changes in antenna characteristics due to physical deformation such as bending caused by the movement of the human body must be considered.

One of the major drawbacks of the wearable flexible antenna is that when the antenna is bent or stretched, the radiation efficiency of the antenna decreases. [8] To improve this, silver flakes embedded silicone [9], [10], silver loaded fluorine rubber [11], CNT based films [12], liquid metals in stretchable

Manuscript received January 25, 2022; revised February 15, 2022 and April 23, 2022; accepted 09 August, 2022. Date of publication xx xx, 202x; date of current version xx xx, 202x. (Dates will be inserted by IEEE; "published" is the date the accepted preprint is posted on IEEE Xplore®; "current version" is the date the typeset version is posted on Xplore®). Corresponding author: Yongtaek Hong (e-mail: Yongtaek@snu.ac.kr). This work was supported by the Technology Innovation Program (RS-2022-00154983, Development of Low-Power Sensors and Self-Charging Power Sources for Self-Sustainable Wireless Sensor Platforms) funded By the Ministry of Trade, industry & Energy (MI, Korea).

Jinhyoung kim, Yongtaek Hong and Jungseok Oh are with the Seoul National University, #1, Gwanak-ro, Gwanak-gu, Seoul, Korea (e-mail: kimjh91@keti.re.kr; yongtaek@snu.ac.kr; jungsuek@snu.ac.kr).

Jinhyoung kim, Kwonhong Lee Cheolung Cha are with the Korea Electronics Technology Institute, #25, Saenari-ro, Bundang-gu, Seongnam-si, Gyeonggi-do, Korea (e-mail: kimjh91@keti.re.kr; zero1194@keti.re.kr; cucha@keti.re.kr).

Fig. 1. Side view of wavy surface antenna with gridded air-gap substrate.

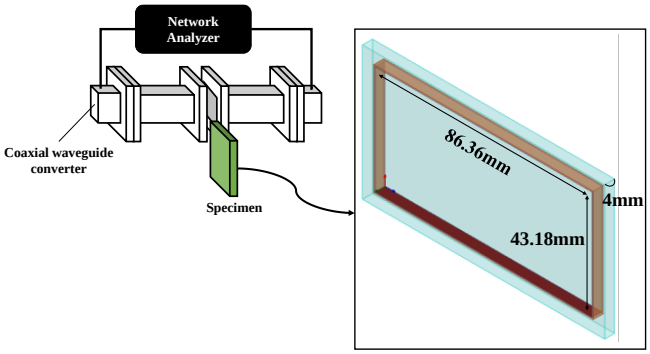

Fig. 2. Form factor of 2.4GHz wave guide for calculating permittivity.

substrate [13], and stretchable fabric [14], Antennas have been manufactured using various materials such as [15].

Another problem is that the resonant frequency shifts when the antenna is bent [16], [17]. In order to improve this, in the existing research, the issue of resonant frequency movement was minimized by fabricating a broadband antenna [18], and a shorting pin was installed between the patch and the ground to minimize the bending effect [19]. In addition, a study on fabricating a flexible reconfigurable antenna using a varactor diode and an external circuit has also been reported [20]-[22]. On the other hand, a paper using it as a sensor rather than improving it was also published [9] and [10].

As mentioned above, the flexible antenna should minimize the rejection of the human body and maintain its electrical characteristics even if physical deformation is applied. In particular, no clear solution has yet been reported for the issue of resonant frequency shift due to physical deformation. Therefore, in this paper, we intend to provide a solution to the issue of resonant frequency shift. In addition, there have been many approaches in terms of materials in the past, but this paper has the advantage of being applicable to flexible antennas of any material because the problem is solved through a structural approach. The fundamental reason for the change of the center frequency is that parasitic such as inductance and capacitance occur when the antenna is bent. That is, if the parasitic components generated before and after the antenna bend can be made the same, the center frequency can be maintained without changing. The structure that makes it possible is the wavy surface structure.

The structure of this paper is as follows. First, in Part 1, the necessity, merits, and design method of a gridded substrate, which is essential to fabricate a wavy surface, are discussed. After that, in Part 2, an analysis method of wavy surface structure using MATLAB was introduced, and it was verified by fabricating a wavy surface antenna using a gridded substrate. In the last part, it was confirmed that frequency correction is possible through an actual power transmission experiment.

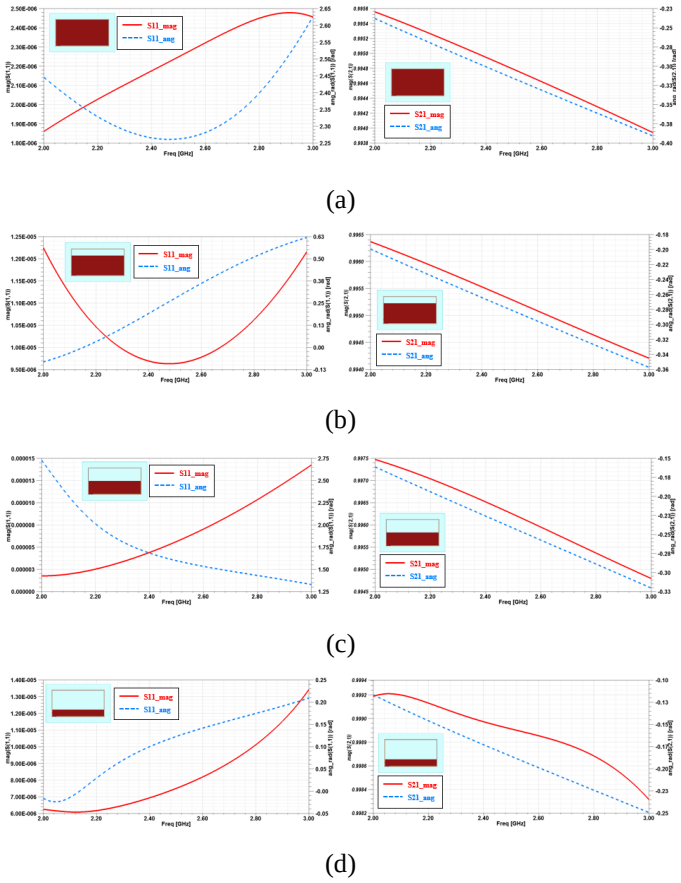

Fig. 3. Changes in s11 magnitude and phase angle according to the ratio of PDMS and air within the operating frequency range of waveguide.

II. Antenna Design using Gridded Substrate

Fig. 1 shows the side view of the wavy surface antenna. As shown in Fig. 1, a wavy structure can be implemented only when there is an empty space between the substrates. Therefore, it is necessary to design an antenna using a gridded substrate in which rod-shaped dielectrics are regularly arranged. For this, research on the high-frequency characteristics of the gridded substrate must be preceded.

A. Waveguide Design to Obtain Dielectric Constant of Gridded Substrate

The transmission phase-shift method was used to understand the high frequency characteristics of the gridded substrate. This method is easy to obtain the dielectric constant and loss-tangent at a specific frequency by using the scattering parameter [23]. As this method basically utilizes the attenuation and phase shift occurring within the waveguide, the waveguide was designed according to the target frequency (2400 MHz) as shown in Fig.

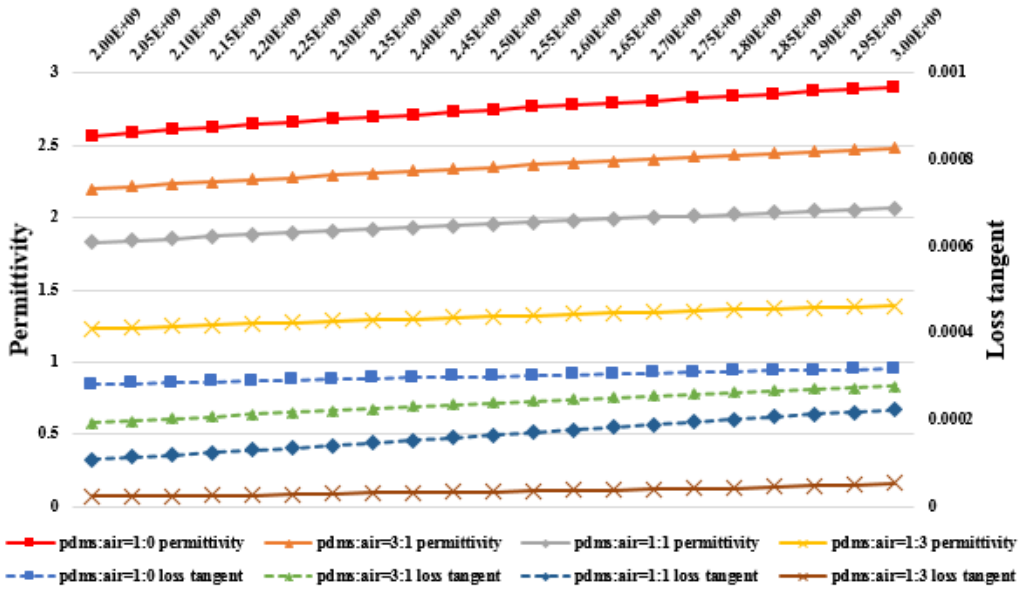

Fig. 4. Changes in permittivity and loss tangent according to PDMS and air ratio within the waveguide's operating frequency range.

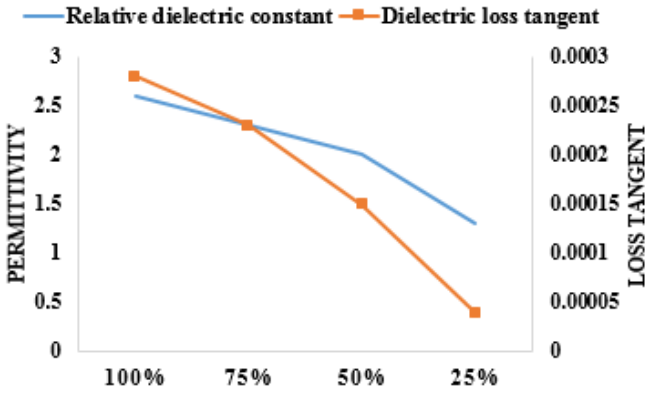

Fig. 5. Changes in permittivity and loss tangent according to PDMS and air ratio.

2. In the designed wave guide, scattering parameters were extracted by varying the ratio of air and PDMS as shown in Fig. 3. The extracted scattering parameter can be calculated as dielectric constant thorough (1) and tangent loss through (2).

$$\varepsilon_r' = \frac{A}{k_0^2}\left\{\left(\sqrt{k_0^2 - \left(\frac{\pi}{a}\right)^2} + \frac{\phi_{21}^{Air} - \phi_{21}^{Sample}}{d_s}\right)^2 + \left(\frac{\pi}{a}\right)^2 - \alpha_s^2\right\} \quad (1)$$

$$\varepsilon_r'' = \frac{2A\alpha_s}{k_0^2}\left(\sqrt{k_0^2 - \left(\frac{\pi}{a}\right)^2} + \frac{\phi_{21}^{Air} - \phi_{21}^{Sample}}{d_s}\right) \quad (2)$$

Where,

$$A = \left(\frac{f}{f_{center}}\right)^{\beta}$$

and

$$\alpha_s \approx -1.15129254\left[\begin{matrix}\log_{10}\left(\left|S_{11}^{Sample}\right|^2 + \left|S_{21}^{Sample}\right|^2\right) \\ -\log_{10}\left(\left|S_{11}^{Air}\right|^2 + \left|S_{21}^{Air}\right|^2\right)\end{matrix}\right]$$

Symbol f is the operating frequencies. The β is a constant value depended on the model and the quality of the rectangular waveguide. In this study, the β was set to 0.3. In fact, the A coefficient is used to improve the imperfection of propagation wave in the region other than the operating frequency.

The calculated permittivity and tangent loss can be expressed according to the frequency within the operating frequency of the waveguide, and the result is shown in Fig. 4. According to Fig. 4, it can be seen that the dielectric constant and tangent loss decrease as the PDMS ratio decreases.

Fig. 5 shows only the result at the design frequency. If the permittivity value is the most important factor influencing the design, it is also a matter of wavelength. When the dielectric constant changes, the wavelength of the electromagnetic wave propagating in the dielectric is divided by the square root of the dielectric constant, that is, has a guided wavelength value, which has a decisive influence on the size of the circuit structure itself. As the dielectric constant decreases, the wavelength increases, and the antenna radiation area increases. Due to this fact and the smaller tangent loss, the gain of the antenna increases. In summary, as the PDMS, that is, the substrate ratio decreases, the antenna gain can be improved.

B. Gridded Substrate Antenna Design.

In this chapter, a monopole antenna and a rectangular patch antenna were designed based on the results obtained above. Both types of antennas were designed using a conventional substrate and a gridded substrate. The antenna was designed in the most basic microstrip patch type. In the case of monopole, the length was set according to the wavelength of 2.4 GHz, and the width was optimized to match 50 ohms. In the case of a rectangular patch antenna, it was designed using (3), (4). And then each length was fine-tuned and optimized.

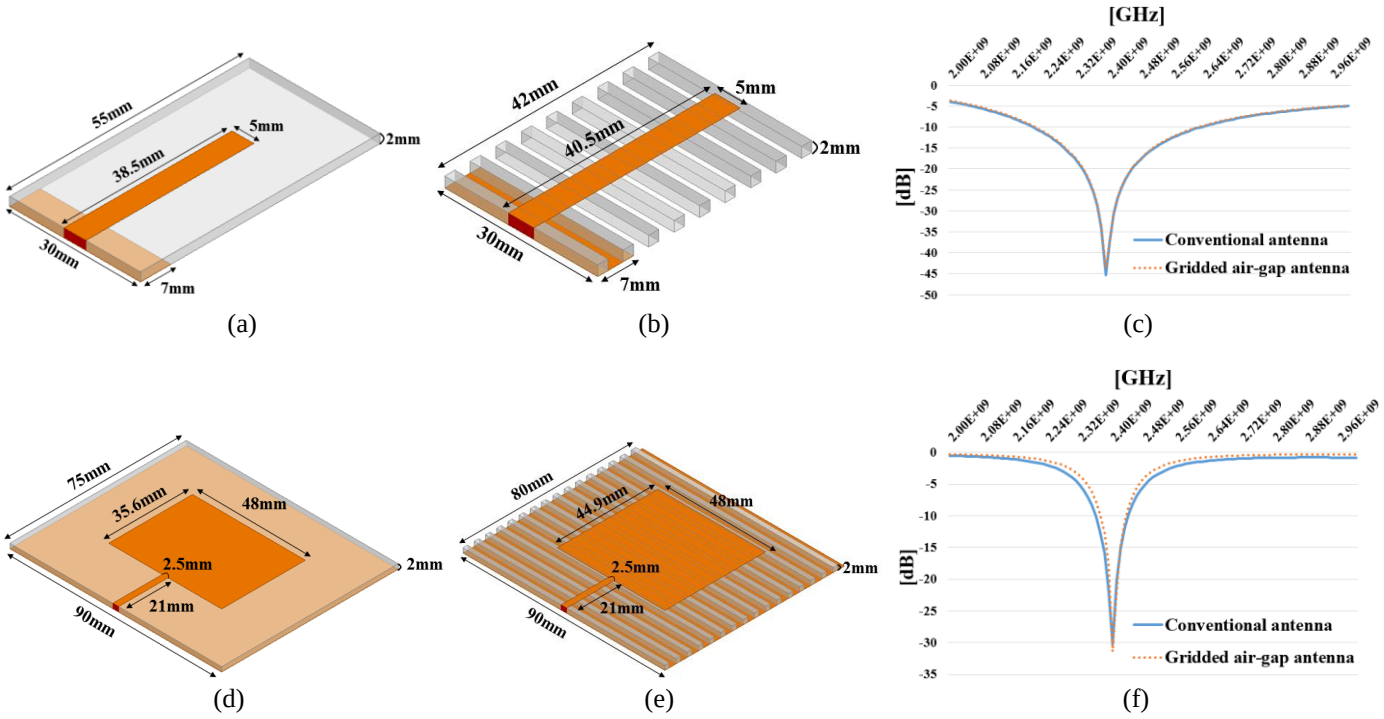

Fig. 6. Comparison of conventional antenna and gridded antenna design results. monopole: (a) conventional antenna, (b) gridded antenna, (c) S11 comparison result, patch: (d) conventional antenna, (e) gridded antenna, (f) S11 comparison result.

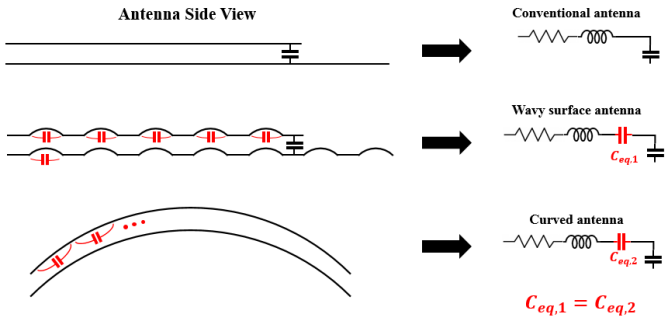

Fig. 7. Conceptual diagram for explaining the parasitic capacitance of the wavy surface antenna.

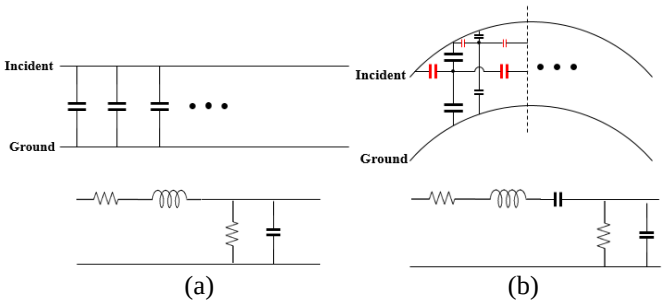

Fig. 8. Equivalent circuit with wavy surface structure in terms of transmission line.

$$\mathrm{w} = \frac{c}{2f_0\sqrt{\frac{(\varepsilon_r+1)}{2}}} \tag{3}$$

$$\mathrm{L} = L_{eff} - 2\Delta L \tag{4}$$

Where,

$$\varepsilon_{eff} = \frac{\varepsilon_r + 1}{2} + \frac{\varepsilon_r - 1}{2}\left[1 + 12\frac{h}{W}\right]^{-\frac{1}{2}}$$

and

$$L_{eff} = \frac{c}{2f_0\sqrt{\varepsilon_{eff}}},\ \Delta\mathrm{L} = 0.412\mathrm{h}\frac{(\varepsilon_{eff}+0.3)\left(\frac{W}{h}+0.264\right)}{(\varepsilon_{eff}-0.258)\left(\frac{W}{h}+0.8\right)}$$

The symbol W is antenna width and the symbol L is antenna length. And c is the propagation velocity in the air, and ε_{eff} and L_{eff} are the effective permittivity and effective length, respectively. Finally, f_0 represents the operating frequency, and h represents the height of the substrate.

As mentioned above, there is a difference in permittivity between a general substrate and a gridded substrate. In the case of a gridded substrate, it is advantageous to minimize the ratio of PDMS, but in this paper, the design was carried out by setting the ratio of PDMS and air to 2:3 for ease of fabrication. In this case, the dielectric constant of the gridded substrate was calculated as 1.7078 and the loss tangent was 1.0089e-0.4, and the design was carried out using these values. And the substrate height, h, is set to 2mm.

The design result of the monopole antenna is shown in Fig. 6 (a)-(c). As can be seen in the Fig. 6 (b), the length of the antenna increased by 2mm and the gain rose from 2.5787 dBi to 2.7513 dBi. In addition, in terms of bandwidth, as shown in Fig. 6 (c), there was no difference. The design result of the rectangular patch antenna is shown in Fig. 6 (d)-(f). As can be seen from the Fig. 6 (e), the length of the antenna increased by

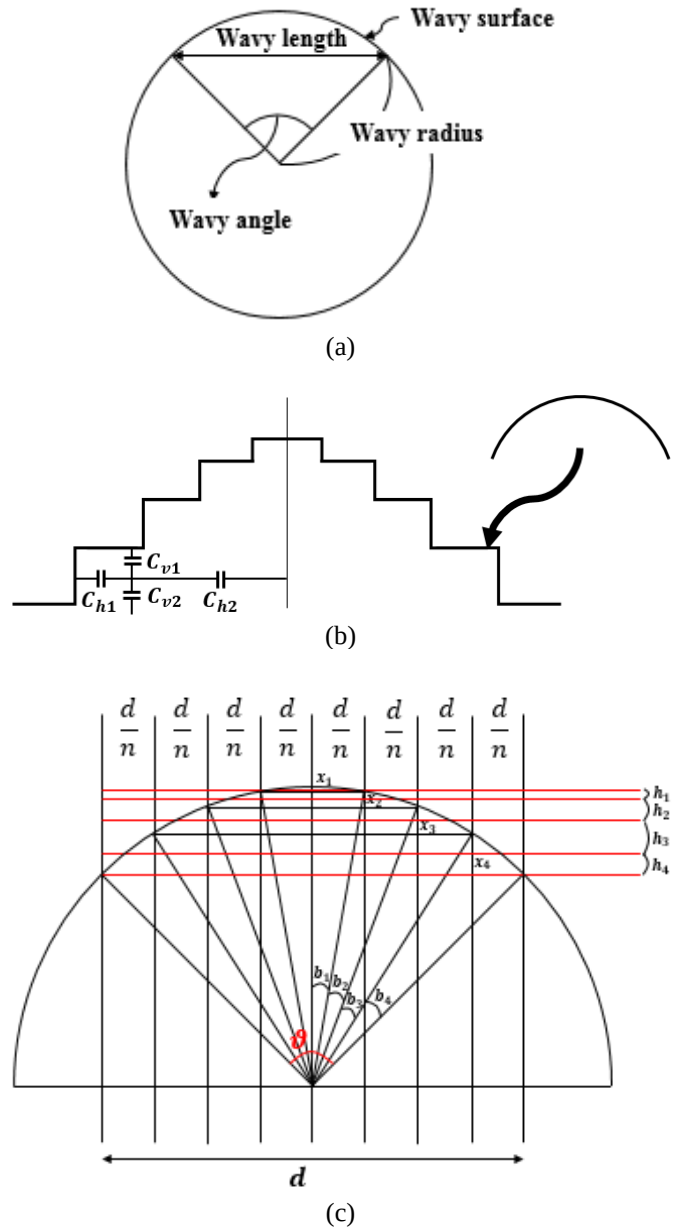

Fig. 9. Mathematical modeling method of wavy surface structure. (a) Setting a variable to mathematicalize a single wavy surface. (b) Simplification of curved surface and setting parasitic capacitance through right angle structure. (c) Depiction of how to set length and angle parameters to calculate parasitic capacitance.

9.3mm, and the gain rose from 4.9307 dBi to 6.3767 dBi. In terms of bandwidth, as shown in Fig. 6 (f), it was about 80 MHz for a general substrate and 75 MHz for a gridded substrate. From this result, it can be seen that high gain can be obtained when using a gridded substrate.

III. Wavy Surface Antenna

A. Wavy Structure Analysis - Parasitic Capacitance

The wavy surface antenna means an antenna that has a curved surface on the antenna surface as shown in Fig. 1. In order to design an antenna that does not change the center frequency, it is necessary to analyze both capacitance and inductance. When the antenna surface is curved, electrical

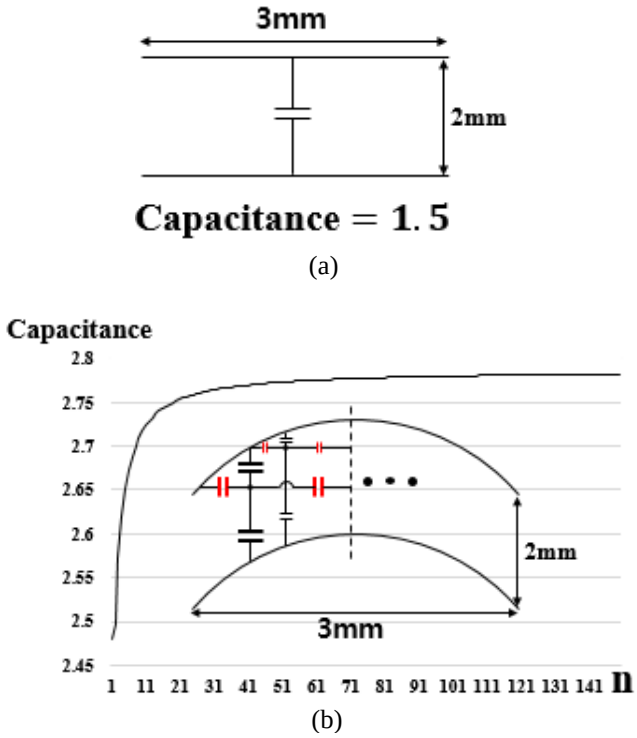

Fig. 10. Comparison of capacitance on a flat surface and on a wavy surface.

parasitic components such as capacitors are generated due to phase difference in the RF environment. In a DC power supply, capacitance does not occur because there is no potential difference in the case of the same node, but in RF, a potential difference occurs due to the phase difference even at the same node, and thus parasitic capacitance may occur.

Through this, the form factor of the antenna having a wavy surface structure can be determined. Also, as shown in Fig. 11, if the total amount of the parasitic capacitance (C_{eq1}) generated on the wavy surface and the parasitic capacitance (C_{eq2}) generated when bending is designed to be the same, it is possible to design an antenna in which the resonance frequency does not change even when bending.

In the case of a general RF line, its characteristics can be described using a transmission line model as shown in Fig. 8 (a), but in the case of an RF line having a radius of curvature as shown in Fig. 8 (b), a modified transmission line model must be applied. At this time, the biggest difference from the existing transmission line model is that a new capacitor component is added. The method of obtaining the capacitance of the wavy structure is as follows.

1. Set the form factor of the target wavy structure. In this paper, wavy radius(r)=2.5 mm, wavy length(d)=3 mm, and substrate height(t)=2 mm. Fig. 9(a) shows the meaning of each variable.

2. In order to calculate the capacitance, one wavy structure was divided into perpendicular components as shown in Fig. 9 (b), and for this, modeling was performed as shown in Fig. 9 (c).

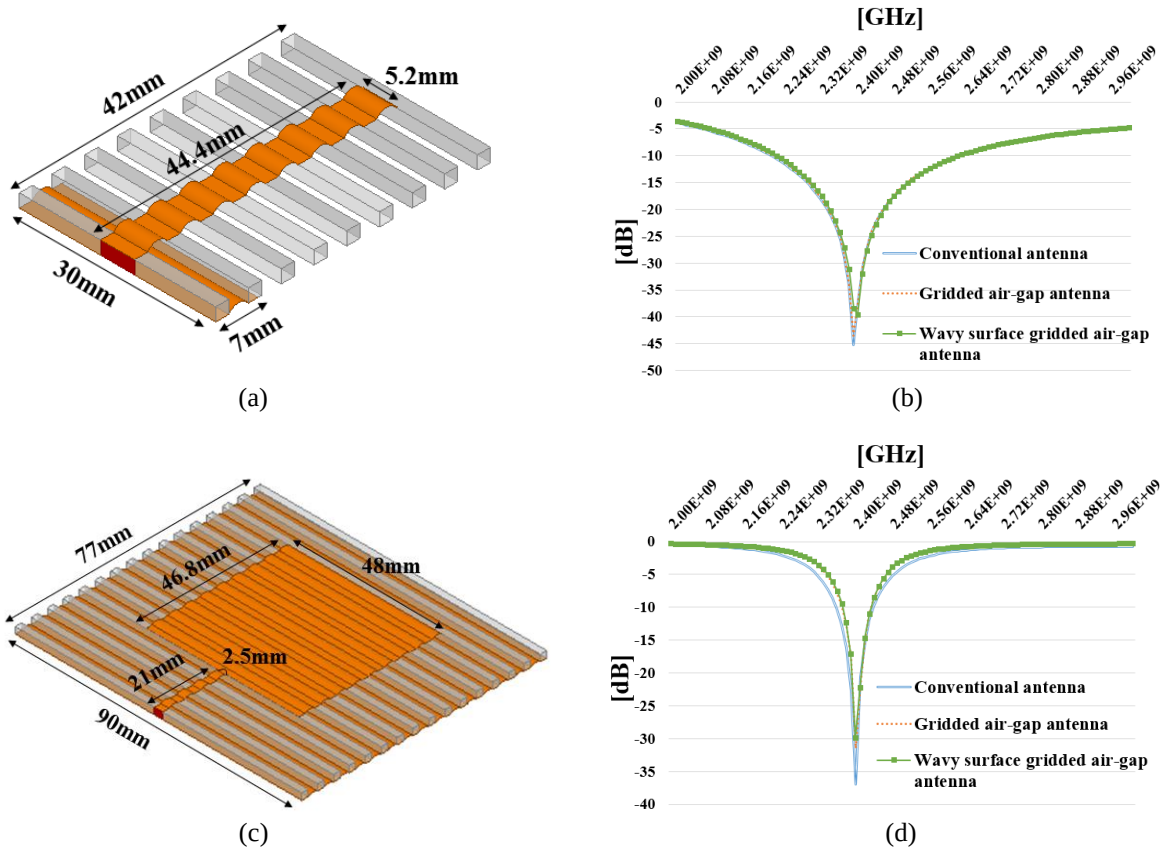

Fig. 11. Wavy surface antenna design results. monopole: (a) wavy surface antenna, (b) S11 comparison result, patch: (c) wavy surface antenna, (d) S11 comparison result.

3. Calculate the differential wavy angle b_m based on the form factor. The formula is as follows.

$$b_m = a_m - a_{m-1}\ (b_0 = 0) \tag{5}$$

Where,

$$a_m = \sin^{-1}\left(\frac{d*m}{n*r}\right)$$

4. Calculate the differential vertical, horizontal length. The linear distance of the wavy structure with the radius of curvature was called d, and it was divided into n differential components. At this time, the differential horizontal length in each divided section was called x_m, and the distance between two adjacent horizontal length was set as h_m. x_m and h_m can be calculated as in (6) and (7), (8) respectively. And the vertical differential length can be calculated by (9).

$$x_m = \frac{d/n}{\tan\left(90-\frac{b_m}{2}-\frac{(m-1)*\theta}{n}\right)} \tag{6}$$

$$h_m = \frac{x_m+x_{m+1}}{2}\left(1 \le m \le \frac{n}{2}-1\right) \tag{7}$$

$$h_m = \frac{x_m}{2}\left(m = \frac{n}{2}\right) \tag{8}$$

$$\mathrm{w} = \frac{d}{n} \tag{9}$$

5. Calculate the differential vertical, horizontal capacitance. (10) and (11) represent differential vertical capacitance, and (12) and (13) are equations for differential horizontal capacitance.

$$c_{v1,m} = \frac{w}{h_m} \tag{10}$$

$$c_{v2,m} = \frac{w}{t-h_m} \tag{11}$$

$$c_{h1,m} = \frac{x_m}{w} \tag{12}$$

$$c_{h2,m} = \frac{x_m \times 2n}{(2m-1)\times d} \tag{13}$$

6. Add up all the calculated capacitances.

$$c_{sum,m} = \frac{(c_{h1}+c_{v1})\times(c_{h2}+c_{v2})}{c_{h1}+c_{h2}+c_{v1}+c_{v2}} \tag{14}$$

If the capacitance is calculated through the above method, the result as shown in Fig. 10(b) can be obtained. Compared to the flat surface capacitance (Fig. 10(a)), it can be seen that it has increased from 1.5 to 2.78. It can be said that the shift of the resonant frequency is observed by this capacitance change amount. Therefore, if the parasitic capacitances c_{eq1} and c_{eq2} are made the same as in Fig. 7 mentioned above, the resonance frequency can be maintained almost the same even if the antenna is bent. In addition, it is possible to determine the form

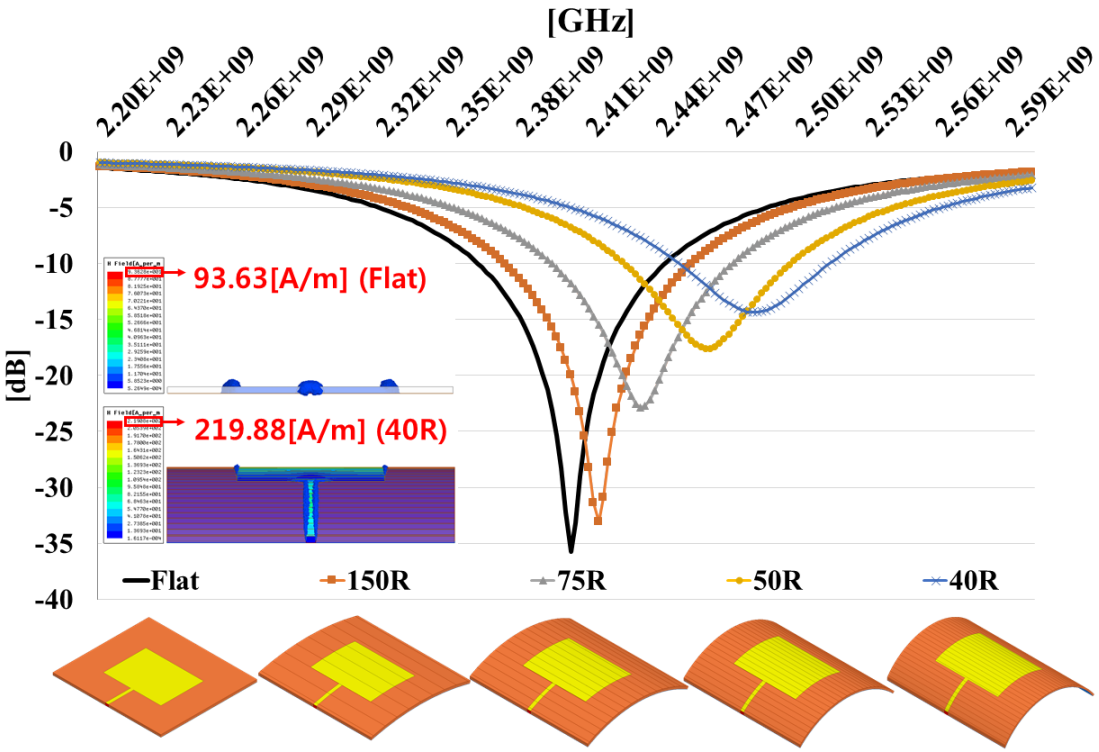

Fig. 12. Center frequency shift and magnetic change according to the degree of antenna bending.

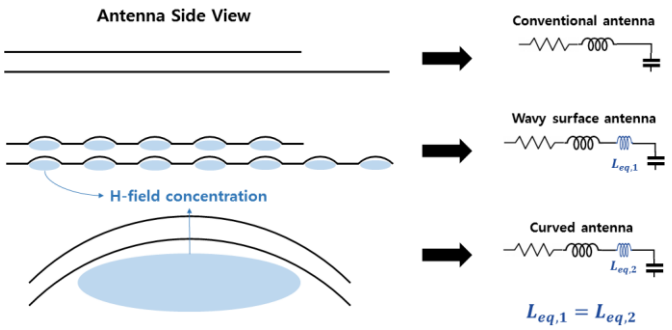

Fig. 13. Conceptual diagram for explaining the parasitic inductance of the wavy surface antenna.

factor of the wavy surface antenna through this result.

B. Wavy Structure Analysis – Parasitic Inductance

In the case of inductance, it can be confirmed by analyzing the H-field. In the Fig. 12, it can be seen that the center frequency shifts when the antenna is bent. At this time, the capacitance also changes, but the amount of change is not large, and the parameter that changes mainly is the inductance. As can be seen from the Fig. 12, in the case of flat, the maximum value of H-field is 93.63 [A/m], but in case of 40R, it is 219.88 [A/m]. As the antenna bends, the field is concentrated inside the antenna and the inductance increases. As shown in Fig. 13, if the inductance, like the capacitance, is the same as the inductance (Leq,1) generated in the wavy surface structure and the inductance (Leq,2) generated in the curved structure, the center frequency can be maintained.

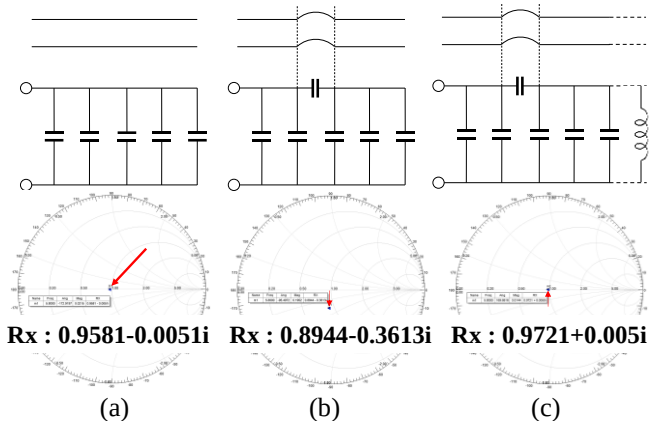

Fig. 14. Equivalent circuit and Smith chart changes when a wavy structure is added.

C. Wavy Surface Antenna Design

Fig. 14 is a circuit in which only the capacitance component is left out of the equivalent circuit of the patch antenna. If there is a wavy surface, it can be seen that capacitance has occurred, as mentioned above. So, the resonant frequency can be corrected by adding an inductance component as shown in Fig. 14(c). The easiest way to add an inductance component in an antenna is to increase the length of the antenna.

When designing a wavy surface antenna through this method, it is shown in Fig. 14. A monopole antenna and a patch antenna were designed, and it can be seen that both have a longer length compared to the conventional flat surface antenna. This is because, as mentioned earlier, the length was increased and optimized to match the resonant frequency to 2.4GHz. In the

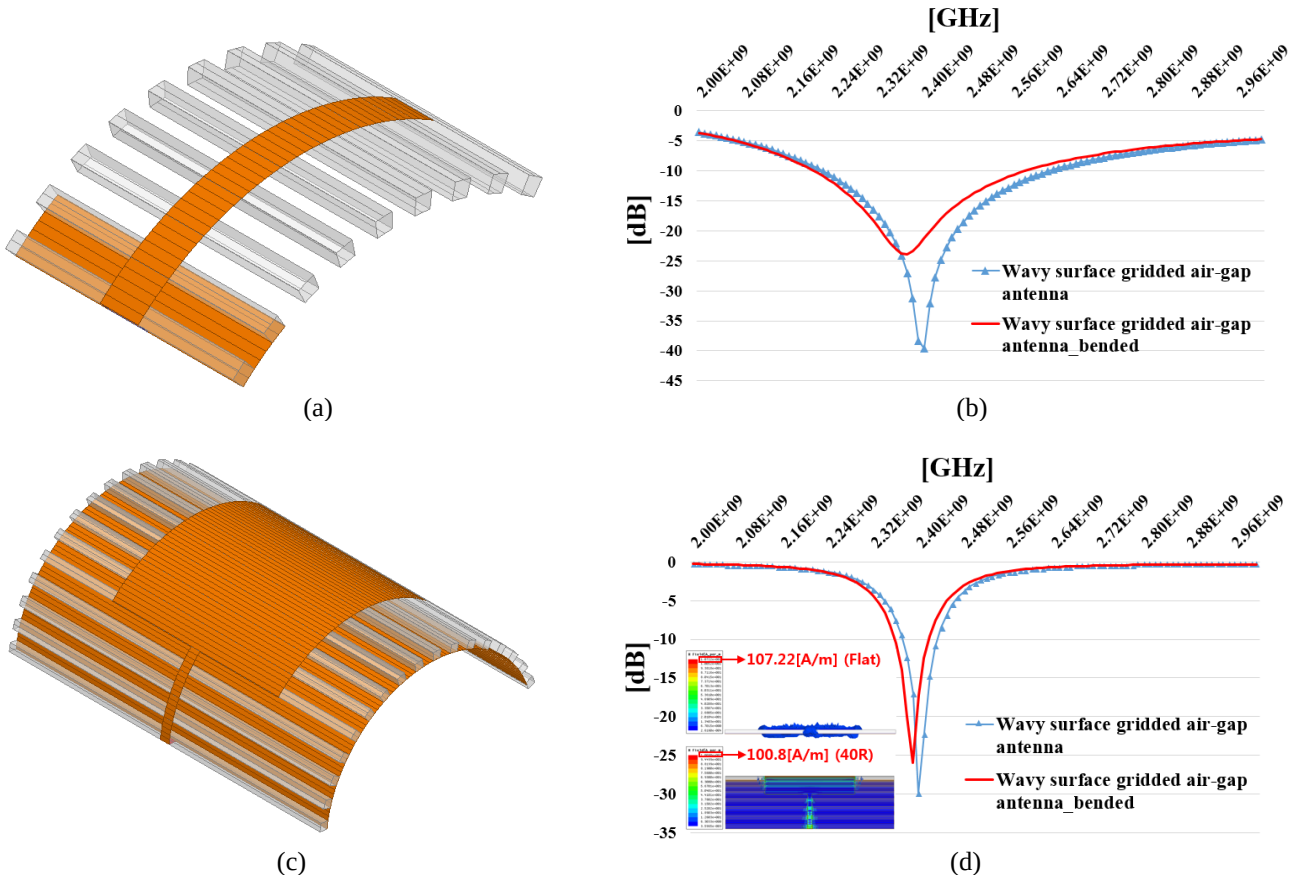

Fig. 15. Bended wavy surface antenna design results. monopole: (a) bended wavy surface antenna (40R), (b) S11 comparison result, patch: (c) bended wavy surface antenna (40R), (d) S11 comparison result.

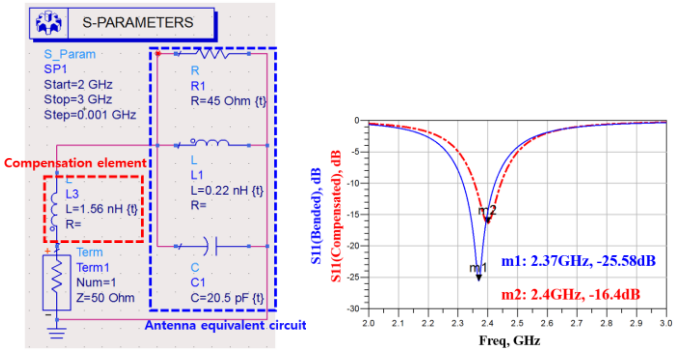

Fig. 16. Frequency reconfiguration circuit simulation (a) Antenna equivalent circuit and passive reconfiguration element, (b) Comparison of s-parameters before and after reconfiguration when the antenna is bent.

case of a monopole antenna, the width of the antenna is also slightly increased, because when a wavy surface is formed, resistance also occurs as a parasitic component. However, this is very small value compared to the capacitance, so it is not considered in this paper.

In the case of the wavy surface patch antenna, it can be seen that the width is similar to that of the flat surface patch antenna, and only the length is slightly increased. In the case of gain, it decreased by 0.0318dB and 0.075dB, respectively, but the amount of decrease was not large. In terms of bandwidth, the monopole antenna showed the same appearance as the previously measured two types of antennas. In the case of the patch antenna, it has a bandwidth of 75 MHz, which is slightly decreased compared to the conventional antenna measured previously.

Fig. 15 shows the simulation result when the wavy surface antenna is bent. This simulation was conducted based on a radius of curvature of 40R. As can be seen in the Fig. 15, when the wavy surface antenna is bent, all the wavy structures existing on the surface are unfolded. At this time, the resonance frequency shifted from 2.4 GHz to 2.37 GHz for a monopole antenna by about 30 MHz, and moved 10MHz from 2.4 GHz to 2.39 GHz for a rectangular patch antenna. The antenna gain decreased slightly from 2.7195 dBi to 2.6135 dBi in the case of a monopole, and decreased from 6.3017 dBi to 5.6699 dBi in the case of a rectangular patch antenna. In addition, it can be seen that the magnitude of the magnetic field before and after bending is almost the same from 107.22 [A/m] to 100.8 [A/m].

In general, antenna characteristics do not vary significantly with E-plane bending. On the other hand, the antenna characteristics according to the H-plane bending are greatly changed. Therefore, existing papers are mainly researching to reconfigure the frequency or gain for the H-plane. This paper is also a study on the H-plane, and the superior reconfiguration characteristics could be confirmed.

Table 1 lists the results compared to previous studies. First, in the case of the resonant frequency, in the case of 39R in the previous paper [19], it shifted about 40 MHz, and in this paper, the monopole and the patch antenna shifted by 30 MHz and 10 MHz, respectively. The difference from the previous paper is

TABLE I
COMPARISON WITH EXISTING PAPERS

Parameters	Conditions	**This work (patch)**	**This work (mono pole)**	B. Hu et al. [19]	Yan. S et al. [24]	Tang, M. C et al. [25]
Realized gain at Res. Freq (dBi)	Flat	**6.3**	**2.72**	1.47	3.9	4.4
	Bending	**5.7**	**2.61**	About -7.5	3.9	3.9
Res. Freq (GHz)	Flat	**2.4**	**2.4**	2.4625	2.45	1.7/1.83
	Bending	**2.39**	**2.37**	2.42	2.422	1.706/1.810
Size(mm^2)	-	**90x77**	**30x42**	70x25	100x100	25x25
Bandwidth (%)	Flat	**3.13**	**16.6**	2.31	5.77	13.4
	Bending	**2.5**	**14.2**	2.6	6.49	12.9
Maximum radius of curvature	-	**30R**	**30R**	39R	40R	50R
Freq reconfiguration circuit	-	**Not necessary**	**Not necessary**	Needed	Used	Used
Real-time reconfiguration	-	**Available**	**Available**	Unavailable	Unavailable	Unavailable

markedly in the antenna gain part. In the previous paper, the realized gain at the resonant frequency was significantly reduced from 1.47 dBi to -7.5 dBi, whereas in this paper, the monopole was slightly reduced from 2.72 dBi to 2.61 dBi and the patch antenna from 6.3 dBi to 5.7 dBi.

In the case of the existing papers [25] and [26], they are the results of research using a frequency reconfiguration circuit. In this case, superior reconfiguration characteristics is shown, but an additional control circuit must be used to control the reconfiguration circuit. The use of a control circuit increases the complexity of the circuit and increases the volume of the system. Also, real-time reconfiguration is not possible without an additional feedback circuit. In this paper, it can be seen that a reconfiguration circuit is unnecessary and real-time reconfiguration is possible by structurally reconfiguring the frequency.

To sum it up, in this paper, the radius of curvature was taken from flat to 40R, and in the case of the conventional antenna, the frequency shift was measured to be 0~3.3% (based on the center frequency) and 0~89% (based on the bandwidth). To overcome this, a wavy surface structure was proposed, and the following differences were obtained. In the case of the proposed antenna, the frequency shift was significantly improved to 0~0.41 % (based on the center frequency) and 0~13 % (based on the bandwidth). In addition, high gain was obtained compared to other papers, and gain loss due to bending was minimized. Finally, since there is no frequency reconfiguration circuit, real-time calibration is possible and the complexity of the sensor system can be reduced. Looking at the results presented in Figure 15, frequency shifting of about 10 MHz (0.41%) still remains, but no additional reconfiguration circuit is required because the degree of movement falls within the bandwidth of the flat antenna. In other words, even if the circuit at the rear end is designed for a flat antenna, the return loss at the center frequency is –17 dBi when bent, which is less than 2 %.

Therefore, when the structure presented in this paper is used, as shown in Table 1 and Figure 19(c), it can be seen that the resonance frequency and realized gain are maintained almost constant without a special circuit depending on the degree of bending. The reason the antenna gain is kept is that the inductance and capacitance are kept constant. In terms of frequency, even in the result presented in Figure 15, frequency shifting of about 10 MHz (0.41 %) still remains, but no additional reconfiguration circuit is required because the degree of movement falls within the bandwidth of the flat antenna. In other words, even if the circuit at the rear end is designed for a flat antenna, the return loss at the center frequency is –17 dBi when bent, which is less than 2 %.

However, if you need accurate frequency reconfiguration, you can solve it with a simple passive component as shown in Figure 16. In order to instantly reconfigure the frequency according to the bending of the antenna, a readout circuit that can read S11, a feedback circuit, and an MCU for feedback are additionally needed. This method is not suitable for wearable systems because of its high complexity and large size. However, the flexible antenna can be used without such a circuit through the wavy surface structure presented in this study.

From the results obtained above, it can be seen that the frequency self-configurable characteristic of the wavy surface antenna can be used in various flexible antenna applications.

D. Fabrication & Test of Wavy Surface Antenna

Fabrication of the wavy surface antenna proceeded as shown in Fig. 17. First, the latex was lengthened, and then a flat surface antenna composed of PDMS and conductive fabric was bonded to the latex using a hot melt film. After that, the increased latex can be reduced again to fabricate a wavy surface antenna. The appearance of the manufactured antenna is shown in Fig 18.

The fabricated antenna was measured through a network analyzer (Agilent E5071a) and a spectrum analyzer (ADVANTEST R3271). In the case of the resonant frequency, it was obtained through the s11 parameter of the network analyzer, and the gain was obtained through the configuration as shown in Fig. 19(a). If you know the transmit distance,

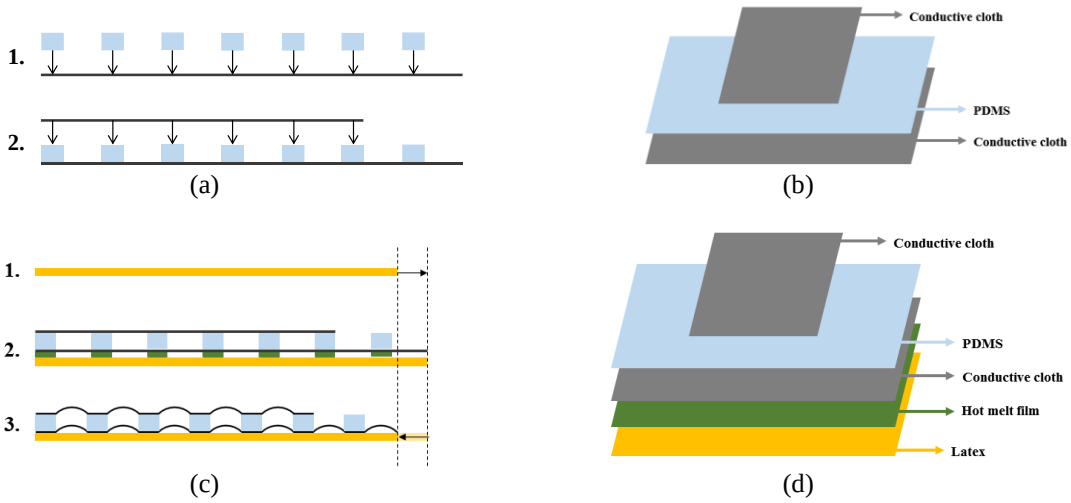

Fig. 17. Conventional patch antenna (a) production sequence, (b) configuration and Wavy surface antenna (c) production sequence, (b) configuration.

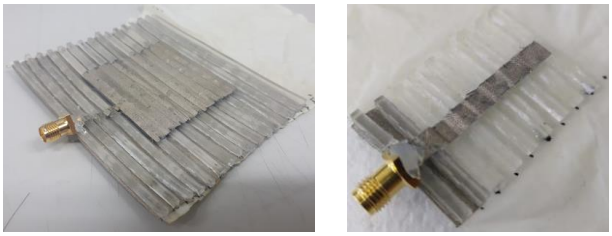

Fig. 18. Fabrication result of monopole wavy surface antenna and patch wavy surface antenna.

transmit and receive power, and transmit antenna gain, you can calculate the receive antenna gain through the friis formula.

$$\frac{P_r}{P_t} = G_r G_r \left(\frac{\lambda}{4\pi R}\right)^2 \tag{13}$$

Experiments are conducted in flat, radius 60mm, and radius 15mm. The above experimental results are shown in Fig. 19 (b). In the case of the existing antenna, it can be seen that the resonant frequency deviates from the operating frequency of 2.4 GHz due to the bending of the antenna. Accordingly, the gain of the antenna at the resonant frequency also significantly decreased. In contrast, it can be confirmed that the wavy surface antenna proposed in this paper maintains the characteristics evenly even when the antenna is bent.

E. Application of Wavy Surface Antenna

Based on the above research results, an experiment was conducted by configuring a wireless power transmission application as shown in Fig. 20. In the transmitting part, the oscillator generates a 2400 MHz signal, amplifies it in the amplifier, and transmits it to the receiving part through the patch antenna. In the receiving part, the gridded antenna is used to receive the transmitted power and then it is transmitted to the LED through the transmission line, the matching network and the rectifier. In this case, the gridded antenna was manufactured in a wavy structure using a conductive cloth without stretchability, and the transmission line was manufactured in a conventional structure using a conductive cloth with stretchability. In the case of a gridded antenna with a wavy

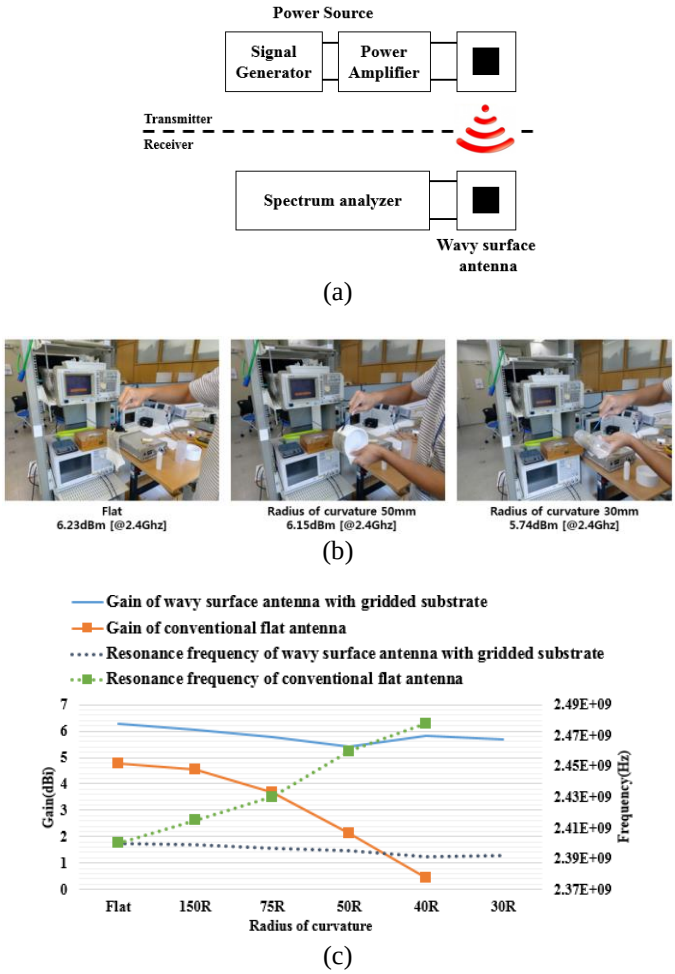

Fig. 18. Power transfer experiment of wavy surface antenna (a) block diagram, (b) experiment in flat, 60R, 30R, (c) result

structure, the characteristics are maintained even when the antenna is bent as mentioned above, but in the case of a transmission line, the characteristics change when the line is bent. In other words, the transmission line can be used as a strain sensor, and a power-free sensor platform as shown in the fig. 20 can be configured by using it together with a gridded antenna.

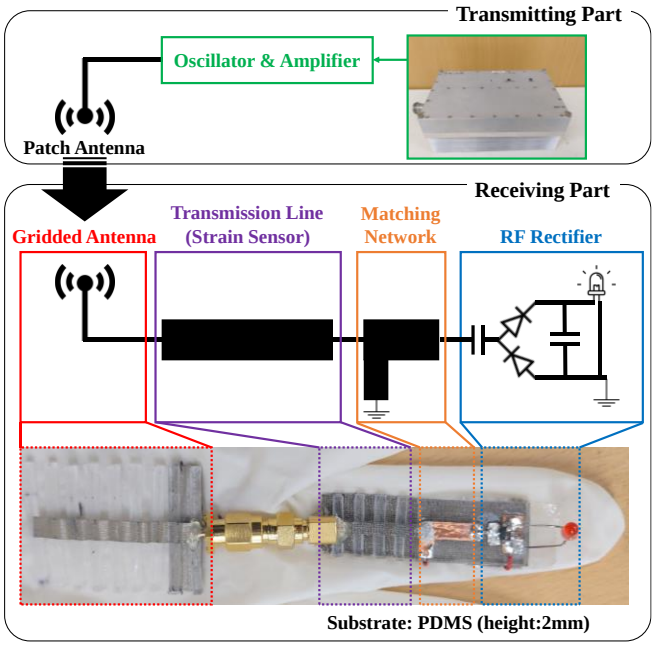

Fig. 20. System configuration for implementing a battery-less sensor platform.

(a)

(b) (c)

Fig. 21. (a) Wireless power transfer experiment of wavy surface antenna and battery-less sensor platform, (b) Result in flat (c) Result in bent.

The experimental results are shown in fig. 21&22. First, the power reception performance was checked at a distance of 1.5 m using a wooden hand model. At this time, in the case of the transmit antenna, a 2x2 array antenna was used for high gain, and the transmit power was set to 3 W. As can be seen from Fig. 20, there was no difference in the brightness of the LED between the case where the antenna was "flat" and the case where the antenna was "bent". For a more detailed experiment, the sensor platform manufactured as in fig. 21 was worn on the hand and the experiment was carried out. First, the experiment was conducted by changing only the angle of the antenna while maintaining the angle of the sensor, and the results are presented in fig. 22(b). As can be seen from the figure, the brightness of the LED according to the bending degree of the antenna was constant. After that, while maintaining the angle of the antenna, only the bending degree of the sensor was changed

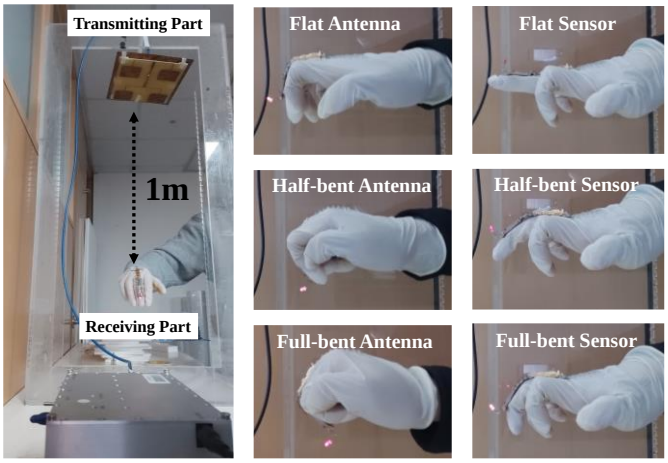

(a) (b) (c)

Fig. 22. (a) Wireless power transfer experiment of wavy surface antenna and battery-less sensor platform, (b) Antenna bending test (c) Sensor bending test.

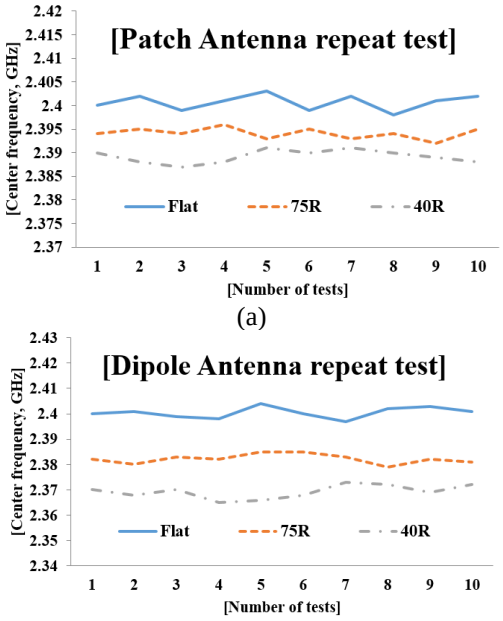

(a)

(b)

Fig. 23. Center frequency repetition test according to bending degree of Wavy surface antenna

and the brightness of the LED was compared, and the result is as fig. 22(c). The brightness of the LED changed according to the bending degree of the sensor, and the LED became brighter as it moved from "flat" to "full-bent". Through this, it can be seen that the brightness of the LED depends only on the bending degree of the sensor. Ultimately, it can be confirmed through the above experiment that this study can be applied to battery-less wearable devices.

F. Stability Test of Wavy Surface Antenna

The center frequency was repeatedly measured while changing the degree of bending of the wavy surface antenna, and the results are shown in Fig. 23. First, in the case of patch antenna, the fluctuation range was within 0.12 % based on 2.4 GHz. Also, in the case of dipole antenna, it was confirmed that the fluctuation range was within 0.15 %. Of course, in actual

use, it can have a larger fluctuation range because there is a part that is bent in an atypical shape, but as mentioned in the introduction, the change in the center frequency according to the bending of the axis belonging to the width of the antenna is not large. Therefore, it is negligible.

IV. Conclusion

In this paper, we proposed an antenna whose frequency is self-reconfigured even when the antenna is curved. In the case of the conventional antenna, when the antenna is bent, the resonant frequency of the antenna is shifted, and accordingly, the antenna gain is greatly reduced. For this reason, conventionally, the issue was solved through a reconfiguration circuit using a varactor diode, and the resonant frequency shift was minimized through material research.

In this paper, we tried to solve this issue by modifying the structure of the antenna, and to this end, a wavy surface antenna was proposed. Through the wavy surface antenna, the deviation of the resonant frequency was reduced to within 0.5%, and the gain of the antenna was also reduced to within 0.5dBi. In addition, it was possible to fabricate an antenna with an improved gain of about 1.446dBi by using a gridded substrate structure. Finally, in this paper, a battery-less wearable sensor platform was proposed to present the scalability of the wavy surface antenna, and its operation was verified by actually manufacturing it. In order to develop wearable sensor technology in the future, the development of power supply technology is essential. In the future, based on the results of this paper, it is predicted that it can be used for the fabrication of a wearable antenna or a sensor-antenna integrated structure.

V. Acknowledgement

This work was supported by the Technology Innovation Program (RS-2022-00154983, Development of Low-Power Sensors and Self-Charging Power Sources for Self-Sustainable Wireless Sensor Platforms) funded By the Ministry of Trade, industry & Energy (MI, Korea).

References

[1] Cisco Visual Networking Index: Global Mobile Data Traffic Forecast Update, 2017–2022, San Jose, CA, USA, 2019, pp. 1–36.
[2] S. Bhattacharyya, N. Das, D. Bhattacharjee and A. Mukherjee, Handbook of Research on Recent Developments in Intelligent Communication Application. Philadelphia, PA, USA: IGI Global, 2016.
[3] M. Chan, D. Estève, J.-Y. Fourniols, C. Escriba, and E. Campo, "Smart wearable systems: Current status and future challenges," Artif. Intell. Med., vol. 56, no. 3, pp. 137–156, Nov. 2012.
[4] Y. Kim et al., "Stretchable nanoparticle conductors with self-organized conductive pathways," Nature, vol. 500, pp. 59–63, Aug. 2013.
[5] P. Nepa and H. Rogier, "Wearable antennas for off-body radio links at VHF and UHF bands: Challenges, the state of the art, and future trends below 1 GHz," IEEE Antennas Propag. Mag., vol. 57, no. 5, pp. 30–52, 2015.
[6] R. Salvado, C. Loss, R. Gonçalves, and P. Pinho, "Textile materials for the design of wearable antennas: A survey," Sensors, vol. 12, no. 11, pp. 15841–15857, 2012.
[7] D. H. Werner and Z. H. Jiang, Electromagnetics of Body Area Networks: Antennas, Propagation, and RF Systems. Hoboken, NJ, USA: Wiley, 2016.
[8] P. Salonen, Y. Rahmat-Samii, M. Schaffrath, and M. Kivikoski, "Effect of textile materials on wearable antenna performance: A case study of GPS antennas," in Proc. IEEE Antennas Propag. Soc. Symp., vol. 1, Jun. 2004, pp. 459–462.
[9] L. Song, A. C. Myers, J. J. Adams, and Y. Zhu, "Stretchable and reversibly deformable radio frequency antennas based on silver nanowires," ACS Appl. Mater. Interfaces, vol. 6, no. 6, pp. 4248–4253, 2014.
[10] T. Rai, P. Dantes, B. Bahreyni, and W. S. Kim, "A stretchable RF antenna with silver nanowires," IEEE Electron Device Lett., vol. 34, no. 4, pp. 544–546, Apr. 2013.
[11] A. Kumar et al., "A highly deformable conducting traces for printed antennas and interconnects: Silver/fluoropolymer composite amalgamated by triethanolamine" Flexible Printed Electron., vol. 2, no. 4, 2017, Art. no. 045001.
[12] G. Xiaohui et al., "Flexible and reversibly deformable radio-frequency antenna based on stretchable SWCNTs/PANI/Lycra conductive fabric" Smart Mater. Struct., vol. 26, no. 10, 2017, Art. no. 105036.
[13] J.-H. So, J. Thelen, A. Qusba, G. J. Hayes, G. Lazzi, and M. D. Dickey, "Reversibly deformable and mechanically tunable fluidic antennas" Adv. Funct. Mater., vol. 19, pp. 3632–3637, Nov. 2009.
[14] M. Park et al., "Highly stretchable electric circuits from a composite material of silver nanoparticles and elastomeric fibres" Nature Nanotechnol., vol. 7, pp. 803–809, Nov. 2012.
[15] R. Ashayer-Soltani, C. Hunt, and O. Thomas, "Fabrication of highly conductive stretchable textile with silver nanoparticles," Textile Res. J., vol. 86, pp. 1041–1049, Sep. 2015.
[16] S. J. Chen, B. Chivers, R. Shepherd, and C. Fumeaux, "Bending impact on a flexible ultra-wideband conductive polymer antenna," in Proc. Int. Conf. Electromagn. Adv. Appl. (ICEAA), 2015, pp. 422–425.
[17] Q. Bai and R. Langley, "Wearable EBG antenna bending and crumpling," in Proc. Loughborough Antennas Propag. Conf., 2009, pp. 201–204.
[18] P. Salonen and Y. Rahimat-Samii, "Textile antennas: Effects of antenna bending on input matching and impedance bandwidth," IEEE Aerosp. Electron. Syst. Mag., vol. 22, no. 3, pp. 10–14, Mar. 2007.
[19] B. Hu, G.-P. Gao, L.-L. He, X.-D. Cong, and J.-N. Zhao, "Bending and on-arm effects on a wearable antenna for 2.45 GHz body area network," IEEE Antennas Wireless Propag. Lett., vol. 15, pp. 378–381, 2016.
[20] X. L. Yang, J. C. Lin, G. Chen, and F. L. Kong, "Frequency reconfigurable antenna for wireless communications using GaAs FET switch," IEEE Antennas Wireless Propag. Lett., vol. 14, no., pp. 807–810, Dec. 2015.
[21] H. Zhai, L. Liu, C. Zhan, and C. Liang, "A frequency-reconfigurable triple-band antenna with lumped components for wireless applications," Microw. Opt. Technol. Lett., vol. 57, pp. 1374–1379, Jun. 2015.
[22] M. W. Young, S. Yong, and J. T. Bernhard, "A miniaturized frequency reconfigurable antenna with single bias, dual varactor tuning," IEEE Trans. Antennas Propag., vol. 63, no. 3, pp. 946–951, Mar. 2015.
[23] K. Y. You, Y. S. Lee, L. Zahid, M. F. A. Malek, K. Y. Lee, E. M. Cheng, N. H. H. Khamis, "Dielectric measurement for low-loss materials using transmission phase-shift method," Jurnal Teknologi, 77(10):69-77, November 2015.
[24] Yan, Sen, and Guy AE Vandenbosch. "Radiation pattern-reconfigurable wearable antenna based on metamaterial structure." IEEE Antennas and wireless propagation Letters 15 (2016): 1715-1718.
[25] Tang, Ming-Chun, et al. "Pattern-reconfigurable, flexible, wideband, directive, electrically small near-field resonant parasitic antenna." IEEE Transactions on Antennas and Propagation 66.5 (2018): 2271-2280.

Jinhyong Kim received his B.S. and M.S. degrees from Dankook University, Korea, in 2013 and Korea University, korea, in 2015, respectively, and he is currently pursuing the Ph.D. degree in electrical engineering with the Seoul National University, korea, focusing on wireless power transfer and flexible antenna. From 2013 to now, he was with Korea Electronics Technology Institute as a hardware research engineer, working on the development of Smart Sensor Research Center.

He is currently a Fellow Researcher in with Korea Electronics Technology Institute. His research areas include mmWave beam focusing/shaping techniques and high gain antenna for wireless power transfer, and flexible antenna for wearable devices.

Cheolung Cha received B.S. in Electrical Engineering, from Korea Univ., Seoul, Korea in 1996 and M.S. and Ph.D. in Electrical and Computer Engineering (ECE) from Georgia Institute of Technology, Atlanta, GA, USA. from 1998 to 2004.

Since 2004, he has worked for Smart Sensor Research Center, Korea Electronics Technology Institute (KETI). Now he is a director. He is also a visiting professor of School of Electrical Engineering, Korea University, Seoul, Korea, from 2008 to present and a secretary in Technical Committee 47 (Semiconductor devices), International Electrotechnical Commission (IEC), Geneva, Switzerland, from 2007 to present.

His research interests are wireless power transfer technologies such as Inductive coupling, Magnetic Resonant coupling, and Microwave- based beam forming and steering for low power wearable and IoT device and sensor applications. His other research topic is radar sensor system.

Dr. Cha received "53rd IEEE ECTC Outstanding Poster Paper Award" in 2004, "SMTA Outstanding Engineer Award" in 2008, "IEC Thomas Edison Award" in 2015, and "Industrial Technology Award and Medal" from Korean Government in 2015.

Kwonhong Lee received his B.S. and M.S. degrees from Dankook University, Korea, in 2016 and Korea University, korea, in 2019, respectively, and he is currently pursuing the Ph.D. degree in electrical engineering with the Korea University, korea, focusing on design of sensor readout integrated circuit. From 2015 to now, he was with Korea Electronics Technology Institute as a hardware and software research engineer, working on the development of Smart Sensor Research Center.

He is currently a Fellow Researcher in with Korea Electronics Technology Institute. His research areas include design of mixed-signal integrated circuit for implantable sensors and machine learning for behavior of farm machinery

Jungsuek Oh received his B.S. and M.S. degrees from Seoul National University, Korea, in 2002 and 2007, respectively, and a Ph.D. degree from the University of Michigan at Ann Arbor in 2012. From 2007 to 2008, he was with Korea Telecom as a hardware research engineer, working on the development of flexible RF devices. In 2012, he was a postdoctoral research fellow in the Radiation Laboratory at the University of Michigan. From 2013 to 2014, he was a staff RF engineer with Samsung Research America, Dallas, working as a project leader for the 5G/millimeter-wave antenna system. From 2015 to 2018, he was a faculty member in the Department of Electronic Engineering at Inha University in South Korea.

He is currently an Associate Professor in the School of Electrical and Computer Engineering, Seoul National University, South Korea. His research areas include mmWave beam focusing/shaping techniques, antenna miniaturization for integrated systems, and radio propagation modeling for indoor scenarios. He is the recipient of the 2011 Rackham Predoctoral Fellowship Award at the University of Michigan. He has published more than 50 technical journal and conference papers, and has served as a technical reviewer for the IEEE Transactions on Antennas and Propagation, IEEE Antenna and Wireless Propagation Letters, and so on. He has served as a TPC member and as a session chair for the IEEE AP-S/USNC-URSI and ISAP. He has been a senior member of IEEE since 2017.

Yongtaek Hong received B.S. and M.S. in Electronics Engineering, from Seoul Nat'l Univ., Seoul, Korea, and Ph.D. in Electrical Engineering from Univ. of Mich., Ann Arbor, MI, USA. From 2003 to 2006, he was a senior research scientist at Display Science & Technology Center, Eastman Kodak Company, Rochester, NY, USA. Since 2006, he has worked for Dept. Elec. & Comp. Eng., Seoul Nat'l Univ., now is a full professor. He was a visiting professor of Dept. Chem. Eng., Stanford University, from 2012 to 2013.

His research interests are printed/flexible/stretchable thin-film devices, display and sensors for wearable and electronic skin applications. Prof. Hong received IEEE EDS "2005 George E. Smith Award", IEEE/IEEK "Young IT Engineer of The Year Award" in 2010, IEC "1906 Award" in 2012, "Industrial Technology of the Month Award" and "KEIT Chairman's Award" from MOTIE of Korean Government in 2014, and 2015, respectively, SNU CoE Shin Yang Engineering Award in 2015, Best Academic Development in Printed & Flexible Electronics Award from IDTechEX Show Printed Electronics USA and 100 Technology Lighting-up Korea in 2025 Award, both in 2017, "Display Day" Korea MOTIE Minister Award in 2018, "Scientist of The Month" Korea MSIT Minster Award in 2019. He is a convenor of IEC TC110 WG8 (Flexible Display Devices), an executive board member of KIDS and SID, chairs of IEEE ED Seoul Chapter and SID Chapter Formation.